Hill, T. L., Cammarano, A., Neild, S. A., & Wagg, D. J. (2015). Relating Backbone Curves to the Forced Responses of Nonlinear Systems. In G. Kerschen (Ed.), Nonlinear Dynamics, Volume 1: Proceedings of the 33rd IMAC, A Conference and Exposition on Structural Dynamics, 2015. (pp. 113-122). (Conference Proceedings of the Society for Experimental Mechanics Series). Springer. DOI: 10.1007/978-3-319-15221-9_9

Relating backbone curves to the forced responses of nonlinear systems

T.L. Hill[1] *, A. Cammarano[1], S.A. Neild[1] and D.J. Wagg[2]

[1] Department of Mechanical Engineering, University of Bristol, Queen's Building, University Walk, Bristol, UK, BS8 1TR

[2] Department of Mechanical Engineering, University of Sheffield, Sir Frederick Mappin Building, Mappin Street, Sheffield, UK, S1 3JD

ABSTRACT

Backbone curves describe the steady-state responses of unforced, undamped systems, therefore they do not directly relate to any specific forcing and damping configuration. Nevertheless, they can be used to understand the underlying dynamics of nonlinear systems subjected to forcing and damping. Building on this concept, in this paper we describe an analytical technique used to predict the onset of internally-resonant modal interactions in an example system. In conjunction with backbone curve analysis, which can be used to predict the possibility of internally-resonant behaviour, this approach provides an analytical tool for understanding and quantifying internally-resonant regions in the forced responses.

Keywords: Backbone curves; Second-order normal forms; Modal analysis; Modal interaction; Modal reduction

Introduction

As many engineering systems becoming increasingly lightweight and flexible, the ability to model the behaviour resulting from nonlinear characteristics is becoming increasingly important. Although there exist many powerful numerical techniques for the modelling of nonlinear dynamical systems, analytical approaches are often more desirable. This is because analytical descriptions can offer greater insight into the mechanisms behind the dynamical behaviour [1], as well as providing efficient tools for procedures such as optimisation [2]. One dynamic phenomenon that is of particular importance in many nonlinear structures is internal resonance. Internal resonance occurs when the response of one underlying linear mode of a system is triggered by the actions of another, and is commonly seen in structures such as cables, beams, membranes and plates [3, 4].

Some of the analytical techniques that are typically employed for the analysis of nonlinear systems include harmonic balancing [5], multiple scales [6], nonlinear normal modes [7, 8] and normal forms [9, 10]. These techniques may be used to describe the responses of unforced, undamped nonlinear systems, referred to here as *backbone curves*. Although these backbone curves can be used to determine the underlying behaviour of the system, they cannot be related to and specific forced response. Furthermore, many analytical approaches cannot be extended to include forcing and damping, whilst with others their inclusion often proves difficult.

In this paper we first show how the backbone curves may be used to determine whether internal resonance may be observed in the system. We then present a method that may be used to predict the

*Address all correspondence to this author - tom.hill@bristol.ac.uk.

onset of internal resonance in forced and damped responses, and describe regions in which internal resonance will be seen.

Second-order normal form technique

The example system

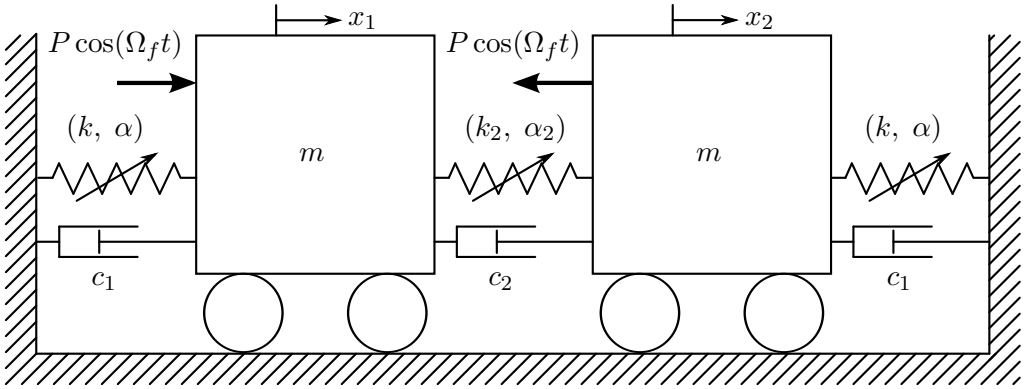

Fig. 1 Schematic of a forced and damped, two-degree-of-freedom, symmetric oscillator with cubic nonlinear springs.

In this paper we consider the forced and damped two-mass nonlinear oscillator shown in Fig. 1 – a system similar to that described in [11]. This system consists of two masses, both of mass m. These masses are connected to ground by two identical cubic nonlinear springs, both with the force-displacement relationship $F = k(\delta x) + \alpha(\delta x)^3$. The masses are also grounded by two identical linear dampers, both with damping constant c. Another cubic nonlinear spring connects the masses, with the force-displacement relationship $F = k_2(\delta x) + \alpha_2(\delta x)^3$, and a linear damper, with damping constant c_2, connects the masses. The displacement of the masses are denoted x_1 and x_2 and are both forced sinusoidally at amplitude P and frequency Ω_f, as shown in Fig. 1. This forcing is in anti-phase, such that the system has a symmetric in structure and applied load.

The equations of motion for this system may be written

$$\mathbf{M}\ddot{\mathbf{x}} + \mathbf{C}\dot{\mathbf{x}} + \mathbf{K}\mathbf{x} + \mathbf{\Gamma}_x(\mathbf{x}) = \mathbf{P}_x \cos(\Omega_f t), \tag{1}$$

where $\mathbf{M}$, $\mathbf{C}$ and $\mathbf{K}$ are the mass, damping and linear stiffness matrices respectively, and $\mathbf{\Gamma}_x(\mathbf{x})$ and $\mathbf{P}_x$ are vectors of the nonlinear terms and forcing amplitudes, written

$$\mathbf{\Gamma}_x(\mathbf{x}) = \begin{pmatrix} \alpha x_1^3 + \alpha_2 (x_1 - x_2)^3 \\ \alpha x_2^3 - \alpha_2 (x_1 - x_2)^3 \end{pmatrix}, \qquad \mathbf{P}_x(\mathbf{x}) = \begin{pmatrix} P_{x1} \\ P_{x2} \end{pmatrix} = \begin{pmatrix} P \\ -P \end{pmatrix}. \tag{2}$$

Applying the second-order normal form technique

We now use the second-order normal form technique to transform the equations of motion, Eq. (1), into a set of time-invariant equations describing the dynamical behaviour. Before applying this technique, we first combine the the damping and nonlinear terms into the vector $\mathbf{N}_x$, allowing us to write Eq. (1) as

$$\mathbf{M}\ddot{\mathbf{x}} + \mathbf{K}\mathbf{x} + \mathbf{N}_x(\mathbf{x}, \dot{\mathbf{x}}) = \mathbf{P}_x \cos(\Omega_f t). \tag{3}$$

The first step of this technique is the linear modal transform, written $\mathbf{x} = \mathbf{\Phi}\mathbf{q}$, where $\mathbf{\Phi}$ is the modeshape matrix, whose n^{th} column describes the modeshape of the n^{th} linear mode. For the system considered

here, the modeshape matrix may be written

$$\mathbf{\Phi} = \begin{bmatrix} 1 & 1 \\ 1 & -1 \end{bmatrix}. \tag{4}$$

Thus, applying this transform to Eq. (3) leads to the modal equation of motion, written

$$\ddot{\mathbf{q}} + \mathbf{\Lambda}\mathbf{q} + \mathbf{N}_q(\mathbf{q}, \dot{\mathbf{q}}) = \mathbf{P}_q \cos(\Omega_f t), \tag{5}$$

where $\mathbf{q}$ is a vector of modal displacements, $\mathbf{N}_q(\mathbf{q}, \dot{\mathbf{q}})$ is a vector of nonlinear and modal damping terms, $\mathbf{P}_q$ is a vector of modal forcing terms and $\mathbf{\Lambda}$ is a diagonal matrix whose n^{th} leading diagonal term is the square of the n^{th} linear natural frequency, ω_{nn}^2. For this system, these may be written

$$\begin{gathered} \mathbf{\Lambda} = \begin{bmatrix} \omega_{n1}^2 & 0 \\ 0 & \omega_{n2}^2 \end{bmatrix} = \frac{1}{m}\begin{bmatrix} k & 0 \\ 0 & k+2k_2 \end{bmatrix}, \qquad \mathbf{P}_q = \begin{pmatrix} P_{q1} \\ P_{q2} \end{pmatrix} = \frac{1}{2m}\begin{pmatrix} P_{x1}+P_{x2} \\ P_{x1}-P_{x2} \end{pmatrix} = \frac{1}{m}\begin{pmatrix} 0 \\ P \end{pmatrix}, \\ \mathbf{N}_q = \begin{pmatrix} 2\zeta_1\omega_{n1}\dot{q}_1 \\ 2\zeta_2\omega_{n2}\dot{q}_2 \end{pmatrix} + \frac{\alpha}{m}\begin{pmatrix} q_1^3 + 3q_1q_2^2 \\ \gamma q_2^3 + 3q_1^2q_2 \end{pmatrix}, \quad \text{where:} \quad \begin{pmatrix} 2\zeta_1\omega_{n1} \\ 2\zeta_2\omega_{n2} \end{pmatrix} = \frac{1}{m}\begin{pmatrix} c \\ c+2c_2 \end{pmatrix}, \end{gathered} \tag{6}$$

where P_{qn} and ζ_n are the linear modal forcing amplitude and modal damping constant of the n^{th} linear mode respectively, and $\gamma = 1 + (8\alpha_2/\alpha)$. Here we assume that the damping constants are equal for both modes, i.e. $\zeta_1 = \zeta_2 = \zeta$, which, from Eq. (6), is true when $\frac{c_2}{c} = \frac{1}{2}\left(\frac{\omega_{n2}}{\omega_{n1}} - 1\right)$.

The system that is considered here may be described by the parameters in Table 1 and we consider the cases where the forcing frequency is in the close vicinity of the linear natural frequencies.

Parameter	m	ω_{n1}	ω_{n2}	α	α_2	ζ	P
Value	1	1	1.005	0.4	0.05	0.004	0.006

Table 1 The parameters describing the example system.

The next step of the second-order normal form technique is the forcing transform, applied to Eq. (5) to give

$$\ddot{\mathbf{v}} + \mathbf{\Lambda}\mathbf{v} + \mathbf{N}_v(\mathbf{v}, \dot{\mathbf{v}}) = \mathbf{P}_v \cos(\Omega_f t). \tag{7}$$

The purpose of this transform is to remove any modal forcing whose frequency is not in the vicinity of the linear natural frequency of the mode on which it is acting. As we are considering forcing frequencies in the vicinity of the linear natural frequencies (which are close – see Table 1), this transform is unity, and we may write

$$\mathbf{q} = \mathbf{v}\,, \qquad \mathbf{N}_q(\mathbf{q}, \dot{\mathbf{q}}) = \mathbf{N}_v(\mathbf{v}, \dot{\mathbf{v}})\,, \qquad \mathbf{P}_q = \mathbf{P}_v\,. \tag{8}$$

The final step of the technique is the nonlinear near-identity transform, written $\mathbf{v} = \mathbf{u} + \varepsilon\mathbf{h}$, where $\mathbf{u}$ and $\mathbf{h}$ are the fundamental and harmonic components of $\mathbf{v}$ respectively. The bookkeeping parameter ε is used to denote that $\mathbf{h}$ is small in comparison with $\mathbf{u}$. Assuming that the fundamental component of the n^{th} linear mode is sinusoidal, we may write

$$u_n = u_{np} + u_{nm} = \frac{U_n}{2}\left(\mathrm{e}^{+\mathrm{j}(\omega_{rn}t - \phi_n)} + \mathrm{e}^{-\mathrm{j}(\omega_{rn}t - \phi_n)}\right), \tag{9}$$

where U_n, ω_{rn} and ϕ_n are the amplitude, response frequency and phase (with respect to the forcing) of the fundamental component of v_n respectively. The subscripts p and m denote the positive and negative (plus and minus) signs of the exponents respectively. As, in the example considered here, the linear natural frequencies are close, we may assume that the response frequencies are equal, i.e. $\omega_{r1} = \omega_{r2} = \Omega$ where Ω is the *common response frequency*.

Along with the harmonics, $\mathbf{h}$. it is also assumed that the nonlinear terms are small, i.e. $\mathbf{N}_v(\mathbf{v}, \dot{\mathbf{v}}) = \varepsilon\mathbf{N}_v(\mathbf{v}, \dot{\mathbf{v}})$. Thus, making the substitution $\mathbf{v} = \mathbf{u} + \varepsilon\mathbf{h}$ into $\varepsilon\mathbf{N}_v(\mathbf{v}, \dot{\mathbf{v}})$ allows us to make the

order ε^1 approximation $\varepsilon\mathbf{N}_v(\mathbf{u}+\varepsilon\mathbf{h},\dot{\mathbf{u}}+\varepsilon\dot{\mathbf{h}}) \approx \varepsilon\mathbf{N}_v(\mathbf{u},\dot{\mathbf{u}})$. From Eqs. (6), (7), (8) and (9) this approximation allows us to write

$$\mathbf{N}_v(\mathbf{u},\dot{\mathbf{u}}) = 2\mathrm{j}\zeta\Omega \begin{pmatrix} \omega_{n1}\left(u_{1p}-u_{1m}\right) \\ \omega_{n2}\left(u_{2p}-u_{2m}\right) \end{pmatrix} + \frac{\alpha}{m} \begin{pmatrix} \left(u_{1p}+u_{1m}\right)^3 + 3\left(u_{1p}+u_{1m}\right)\left(u_{2p}+u_{2m}\right)^2 \\ 3\left(u_{1p}+u_{1m}\right)^2\left(u_{2p}+u_{2m}\right) + \gamma\left(u_{2p}+u_{2m}\right)^3 \end{pmatrix}. \tag{10}$$

The nonlinear near-identity transform results in the resonant equation of motion, written

$$\ddot{\mathbf{u}} + \mathbf{\Lambda}\mathbf{u} + \mathbf{N}_u(\mathbf{u},\dot{\mathbf{u}}) = \mathbf{P}_u\cos(\Omega_f t), \tag{11}$$

where $\mathbf{N}_u(\mathbf{u},\dot{\mathbf{u}})$ is a vector of resonant nonlinear and damping terms and $\mathbf{P}_u = \mathbf{P}_v$. The n^{th} element of the vector $\mathbf{N}_u(\mathbf{u},\dot{\mathbf{u}})$ is populated with the terms from the n^{th} element of $\mathbf{N}_v(\mathbf{u},\dot{\mathbf{u}})$ that are resonant with the n^{th} mode. As, in the example considered here, both modes resonate at the common response frequency, Ω, $\mathbf{N}_u$ is populated with terms that resonate at Ω. The response frequency of the terms in $\mathbf{N}_v$ is determined by defining the vector $\mathbf{u}^*$ which contains all unique combinations of u_{np} and u_{nm} that appear in $\mathbf{N}_v(\mathbf{u},\dot{\mathbf{u}})$. As, from Eq. (10), $\mathbf{N}_v(\mathbf{u},\dot{\mathbf{u}})$ contains 24 unique terms, $\mathbf{u}^*$ is a $\{24\times1\}$ vector. We also define the $\{2\times24\}$ coefficient matrices $[n_v]$ and $[n_u]$, that allow us to write

$$\mathbf{N}_v = [n_v]\mathbf{u}^* \qquad \text{and} \qquad \mathbf{N}_u = [n_u]\mathbf{u}^*. \tag{12}$$

The ℓ^{th} element of $\mathbf{u}^*$ may be written

$$u^*_\ell = \prod_{k=1}^{2} u_{kp}^{s_{\ell kp}} u_{kp}^{s_{\ell km}}, \tag{13}$$

where $s_{\ell kp}$ and $s_{\ell km}$ are the exponents of the u_{kp} and u_{km} in u^*_ℓ respectively. Using these, we may calculate the $\{2\times24\}$ matrix $\boldsymbol{\beta}$, whose $\{n,\,\ell\}^{\text{th}}$ element may be calculated using

$$\beta_{n\ell} = \left(\left[\sum_{k=1}^{2}\left\{s_{\ell kp}-s_{\ell km}\right\}\omega_{rk}\right]^2 - \omega_{rn}^2\right) = \left(\left[\sum_{k=1}^{2}\left\{s_{\ell kp}-s_{\ell km}\right\}\right]^2 - 1\right)\Omega^2. \tag{14}$$

The elements in $\boldsymbol{\beta}$ with a value of zero correspond to elements in $[n_v]$ that describe the coefficients of resonant terms. Thus, in order to populate $\mathbf{N}_u$ with resonant terms, we use

$$n_{u,n\ell} = \begin{cases} n_{v,n\ell} & \text{if} \quad \beta_{n\ell} = 0, \\ 0 & \text{if} \quad \beta_{n\ell} \neq 0. \end{cases} \tag{15}$$

The non-zero elements in $\boldsymbol{\beta}$ correspond to coefficients that are used to describe the harmonics. As we are assuming the harmonics to be negligible here, this step is neglected, however for details of this see [12].

Using Eqs. (10), (13), (14) and (15), we may calculate $[n_v]$, $\mathbf{u}^*$ and $\boldsymbol{\beta}$ as

$$[n_v]^T = \frac{\alpha}{m}\begin{bmatrix} \kappa_1 & 0 \\ -\kappa_1 & 0 \\ 1 & 0 \\ 3 & 0 \\ 3 & 0 \\ 1 & 0 \\ 3 & 0 \\ 6 & 0 \\ 3 & 0 \\ 3 & 0 \\ 6 & 0 \\ 3 & 0 \\ 0 & \kappa_2 \\ 0 & -\kappa_2 \\ 0 & 3 \\ 0 & 3 \\ 0 & 6 \\ 0 & 6 \\ 0 & 3 \\ 0 & 3 \\ 0 & \gamma \\ 0 & 3\gamma \\ 0 & 3\gamma \\ 0 & \gamma \end{bmatrix}, \quad \mathbf{u}^* = \begin{bmatrix} u_{1p} \\ u_{1m} \\ u_{1p}^3 \\ u_{1p}^2 u_{1m} \\ u_{1p} u_{1m}^2 \\ u_{1m}^3 \\ u_{1p} u_{2p}^2 \\ u_{1p} u_{2p} u_{2m} \\ u_{1p} u_{2m}^2 \\ u_{1m} u_{2p}^2 \\ u_{1m} u_{2p} u_{2m} \\ u_{1m} u_{2m}^2 \\ u_{2p} \\ u_{2m} \\ u_{1p}^2 u_{2p} \\ u_{1p}^2 u_{2m} \\ u_{1p} u_{1m} u_{2p} \\ u_{1p} u_{1m} u_{2m} \\ u_{1m}^2 u_{2p} \\ u_{1m}^2 u_{2m} \\ u_{2p}^3 \\ u_{2p}^2 u_{2m} \\ u_{2p} u_{2m}^2 \\ u_{2m}^3 \end{bmatrix}, \quad \boldsymbol{\beta}^T = \Omega^2 \begin{bmatrix} 0 & - \\ 0 & - \\ 8 & - \\ 0 & - \\ 0 & - \\ 8 & - \\ 8 & - \\ 0 & - \\ 0 & - \\ 0 & - \\ 0 & - \\ 8 & - \\ - & 0 \\ - & 0 \\ - & 8 \\ - & 0 \\ - & 0 \\ - & 0 \\ - & 0 \\ - & 8 \\ - & 8 \\ - & 0 \\ - & 0 \\ - & 8 \end{bmatrix}, \tag{16}$$

where $\kappa_1 = \mathrm{j}2\zeta\Omega\omega_{n1}(m/\alpha)$ and $\kappa_2 = \mathrm{j}2\zeta\Omega\omega_{n2}(m/\alpha)$. The elements in $\boldsymbol{\beta}$ that contain a dash $(-)$ correspond to elements in $[n_v]$ that contain a zero, thus are of no importance.

We may now identify the coefficients of resonant terms in $[n_v]$ as those elements that correspond to a zero in $\boldsymbol{\beta}$. Once we have used Eq. (16) to populate $[n_u]$ we can use Eq. (12) to find N_u as

$$\mathbf{N}_u = 2\zeta \begin{pmatrix} \omega_{n1}\dot{u}_1 \\ \omega_{n2}\dot{u}_2 \end{pmatrix} + \frac{3\alpha}{m} \begin{pmatrix} u_{1p}u_{1m}u_1 + 2u_{2p}u_{2m}u_1 + u_{1p}u_{2m}^2 + u_{1m}u_{2p}^2 \\ \gamma u_{2p}u_{2m}u_2 + 2u_{1p}u_{1m}u_2 + u_{1p}^2 u_{2m} + u_{1m}^2 u_{2p} \end{pmatrix}. \tag{17}$$

We may the substitute Eq. (17) into Eq. (11) to find the reonant equation of motion, in which all terms resonate at the common response frequency, Ω.

Finding the backbone curves of the example system

Backbone curves describe the unforced, undamped responses of a system. Therefore, the backbone curves of the example system may be found using the resonant equation of motion, Eq. (11), when the forcing and damping is set to zero, i.e. $\zeta = 0$ and $\mathbf{P}_u^T = [0,\, 0]$. From Eqs. (11) and (17) this leads to

$$\boldsymbol{\Lambda}\mathbf{u} - \Omega^2\mathbf{u} + \frac{3\alpha}{m} \begin{pmatrix} u_{1p}u_{1m}u_1 + 2u_{2p}u_{2m}u_1 + u_{1p}u_{2m}^2 + u_{1m}u_{2p}^2 \\ \gamma u_{2p}u_{2m}u_2 + 2u_{1p}u_{1m}u_2 + u_{1p}^2 u_{2m} + u_{1m}^2 u_{2p} \end{pmatrix} = 0\,. \tag{18}$$

It can be seen, from Eq. (9), that Eq. (18) may be written

$$\boldsymbol{\Upsilon}^+ \mathrm{e}^{+\mathrm{j}\Omega t} + \boldsymbol{\Upsilon}^- \mathrm{e}^{-\mathrm{j}\Omega t} = 0\,, \tag{19}$$

where $\boldsymbol{\Upsilon}^+$ and $\boldsymbol{\Upsilon}^-$ are complex conjugates. Therefore, it is determined that $\boldsymbol{\Upsilon}^+ = 0$, which may be written

$$\boldsymbol{\Upsilon}^+ = \frac{1}{2} \begin{pmatrix} \left[\omega_{n1}^2 - \Omega^2 + \dfrac{3\alpha}{4m}\left\{ U_1^2 + U_2^2\left(2 + \mathrm{e}^{+\mathrm{j}2(\phi_1 - \phi_2)}\right)\right\}\right] U_1 \mathrm{e}^{-\mathrm{j}\phi_1} \\ \left[\omega_{n2}^2 - \Omega^2 + \dfrac{3\alpha}{4m}\left\{\gamma U_2^2 + U_1^2\left(2 + \mathrm{e}^{-\mathrm{j}2(\phi_1 - \phi_2)}\right)\right\}\right] U_2 \mathrm{e}^{-\mathrm{j}\phi_2} \end{pmatrix} = 0\,, \tag{20}$$

which may be simplified to

$$\left[\omega_{n1}^2 - \Omega^2 + \frac{3\alpha}{4m}\left\{\ U_1^2 + U_2^2\left(2 + \mathrm{e}^{+\mathrm{j}2(\phi_1 - \phi_2)}\right)\right\}\right] U_1 = 0\,, \tag{21a}$$

$$\left[\omega_{n2}^2 - \Omega^2 + \frac{3\alpha}{4m}\left\{\gamma U_2^2 + U_1^2\left(2 + \mathrm{e}^{-\mathrm{j}2(\phi_1 - \phi_2)}\right)\right\}\right] U_2 = 0\,. \tag{21b}$$

The imaginary parts of Eqs. (21) both lead to $\sin\left(2|\phi_1 - \phi_2|\right) = 0$. Therefore we may determine that

$$\mathrm{e}^{\mathrm{j}2|\phi_1 - \phi_2|} = \cos\left(2|\phi_1 - \phi_2|\right) = \pm 1 = p. \tag{22}$$

Therefore, if $p = +1$, the fundamental components of the two linear modes are in-phase or in anti-phase, and if $p = -1$ the fundamental components are $\pm 90°$ out-of-phase. In [1] it is shown that $p = -1$ is not a valid solution for the parameters used here, hence substituting $p = +1$ into Eqs. (21) leads to

$$\left[\omega_{n1}^2 - \Omega^2 + \frac{3\alpha}{4m}\left\{\ U_1^2 + 3U_2^2\right\}\right] U_1 = 0\,, \tag{23a}$$

$$\left[\omega_{n2}^2 - \Omega^2 + \frac{3\alpha}{4m}\left\{\gamma U_2^2 + 3U_1^2\right\}\right] U_2 = 0\,. \tag{23b}$$

Aside from the trivial solution in which $U_1 = U_2 = 0$, corresponding to no motion, there exists two solutions in which $U_2 = 0$ and $U_1 = 0$ independently. These single-mode solutions are denoted *S1* and *S2* and are described by

$$\textit{S1}: \qquad U_2 = 0\,, \quad \Omega^2 = \omega_{n1}^2 + \frac{3\alpha}{4m}U_1^2\,, \tag{24}$$

$$\textit{S2}: \qquad U_1 = 0\,, \quad \Omega^2 = \omega_{n2}^2 + \frac{3\alpha\gamma}{4m}U_2^2\,. \tag{25}$$

There also exists two solutions in which U_1 and U_2 are non-zero simultaneously. These solutions, denoted $S3^+$ and $S3^-$ (or $S3^\pm$ when referring to both), have identical frequency-amplitude relationships given by

$$S3^\pm: \qquad U_1^2 = \left(1 - 4\frac{\alpha_2}{\alpha}\right)U_2^2 - \frac{2m}{3\alpha}\left(\omega_{n2}^2 - \omega_{n1}^2\right), \tag{26a}$$

$$\Omega^2 = \frac{3\omega_{n1}^2 - \omega_{n2}^2}{2} + \frac{3(\alpha - \alpha_2)}{m}U_2^2\,. \tag{26b}$$

However, from Eq. (22), the backbone curves $S3^+$ and $S3^-$ correspond to solutions in which u_1 and u_2 are in-phase and in anti-phase respectively. This may be written as

$$S3^+: \quad |\phi_1 - \phi_2| = 0\,, \qquad\qquad S3^-: \quad |\phi_1 - \phi_2| = \pi\,. \tag{27}$$

Figure 2 shows the backbone curves along with the forced response of this system. The backbone curves are represented by light-blue and dashed-red lines for the stable and unstable sections respectively (where the stability has been calculated using the method described in [13]). A light-blue dot shows a bifurcation on *S2*, leading to the branches $S3^\pm$ and an unstable section of *S2*. As *S2* is composed only of u_2, see Eq. (25), and $S3^\pm$ are composed of both u_1 and u_2, this bifurcation is representative of the onset of an internal resonance between the first and second linear modes. Further discussion of this bifurcation is given in [11]. The stable and unstable forced responses are shown by solid-blue and solid-red lines respectively. Additionally, black asterisks represent fold bifurcations and large-red dots show the bifurcations from the second-mode-only forced response branch onto the mixed-mode branch. These forced responses have been calculated using the numerical continuation software AUTO-07p [14], which also provides the stability of the branches and the bifurcations.

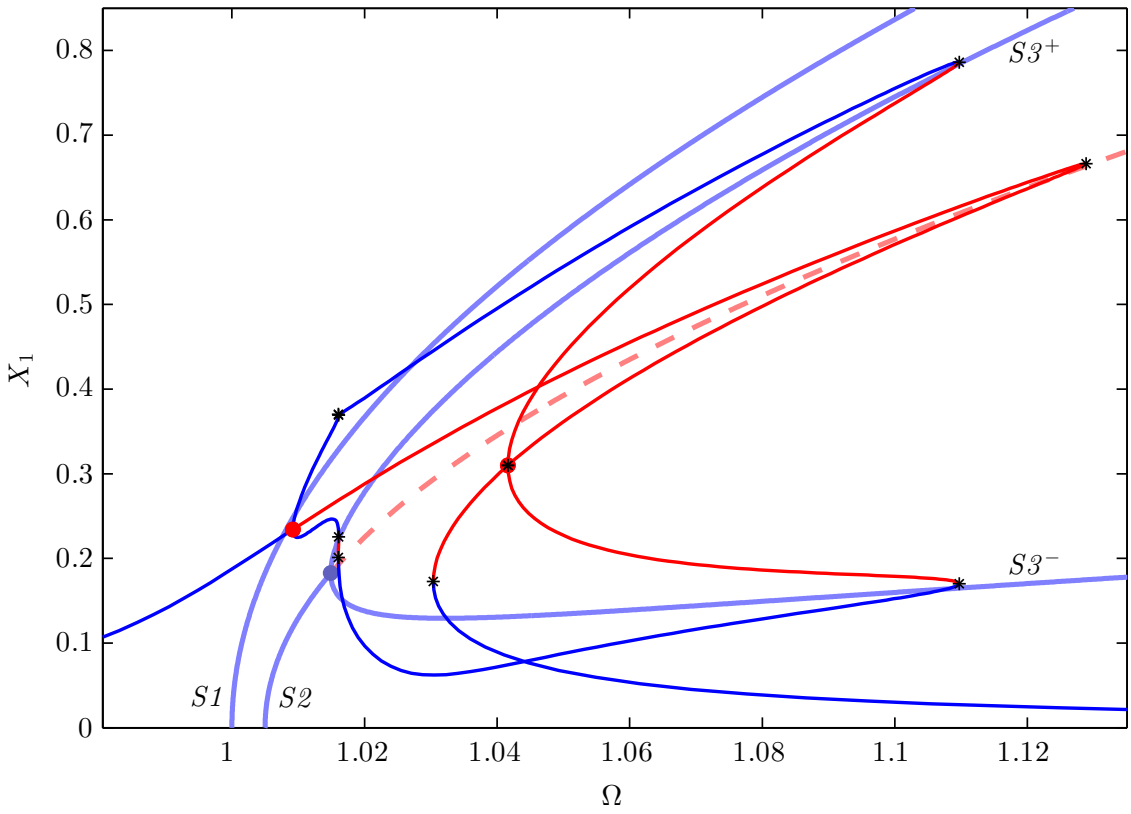

Fig. 2 The backbone curves and forced responses for the example system. This is shown in the projection of the forcing frequency, Ω, against the amplitude of displacement of the first mass, X_1. Solid-blue and solid-red lines show stable and unstable forced responses respectively. Light-blue and dashed-red lines show the stable and unstable backbone curves respectively. Large-red dots show the bifurcations from the second-mode-only forced response onto the mixed-mode forced response and black asterisks represent fold bifurcations. A light-blue dot shows the pitchfork bifurcation from the backbone curve *S2*, onto $S3^{\pm}$.

Figure 2 clearly demonstrates the relationship between the backbone curves and the forced responses of this system. It can be seen that the second-mode-only Duffing-like forced branch envelops *S2* (a second-mode-only backbone curve). Additionally, the bifurcation on *S2* that leads to the mixed-mode backbone curves $S3^{\pm}$ is similar to the bifurcations on the second-mode-only forced branch that leads to mixed-mode forced branches, and these mixed-mode branches also tend-towards $S3^{\pm}$. This relationship shows that the backbone curves may be used to determine whether internal resonance may be seen in a particular structure. However, backbone curves alone cannot be used to determine whether internal resonance will be triggered for a given forcing and damping, or where the onset of internal resonance will be seen. The following section describes an analytical approach that may be used to describe the onset of internal resonance.

Internal resonance

Internal resonance occurs when a non-directly excited (NDE) linear mode exhibits a response. In Eq. (6) it can be seen that the forcing is only applied to the second linear mode (i.e. the first mode is NDE). Through backbone curve analysis we can determine whether multiple-mode solutions exist, such as $S3^{\pm}$ in the example system. Understanding the onset of internal resonance helps to provide insight into the mechanisms behind the forced responses of a system and may be used, for example, to aid the process of

modal reduction as we are able to define if and when particular interactions become significant.

Internal resonance in the example system

Internal resonance may be defined as an instability of the zero-amplitude solution of an NDE mode. To determine the stability of a zero-solution, a similar approach to that taken in [13] may be used. First, we allow the amplitude and phase of the NDE mode to vary slowly with time. For the system considered here this is denoted $U_1 = U_1(\varepsilon t)$ and $\phi_1 = \phi_1(\varepsilon t)$, such that we may write

$$u_1 = u_{1p} + u_{1m} = U_{1p}(\varepsilon t)\mathrm{e}^{+\mathrm{j}\Omega t} + U_{1m}(\varepsilon t)\mathrm{e}^{-\mathrm{j}\Omega t}\,, \tag{28}$$

where the complex conjugates $U_{1p}(\varepsilon t)$ and $U_{1m}(\varepsilon t)$ may be written

$$U_{1p}(\varepsilon t) = \frac{1}{2}U_1(\varepsilon t)\mathrm{e}^{-\mathrm{j}\phi_1(\varepsilon t)}\,, \qquad U_{1m}(\varepsilon t) = \frac{1}{2}U_1(\varepsilon t)\mathrm{e}^{+\mathrm{j}\phi_1(\varepsilon t)}\,. \tag{29}$$

Using Eq. (28) we write the first and second time derivatives of u_1 as

$$\dot{u}_1 = \mathrm{j}\Omega\left(U_{1p}\mathrm{e}^{+\mathrm{j}\Omega t} - U_{1m}\mathrm{e}^{-\mathrm{j}\Omega t}\right) + \mathcal{O}(\varepsilon^1)\,, \tag{30a}$$

$$\ddot{u}_1 = \mathrm{j}\varepsilon 2\Omega\left(U'_{1p}\mathrm{e}^{+\mathrm{j}\Omega t} - U'_{1m}\mathrm{e}^{-\mathrm{j}\Omega t}\right) - \Omega^2 u_1 + \mathcal{O}(\varepsilon^2)\,, \tag{30b}$$

where $\bullet' = \frac{\mathrm{d}\bullet}{\mathrm{d}(\varepsilon t)}$ and Eqs. (30a) and (30b) are truncated at order ε^0 and ε^1 respectively. As $\dot{u}_1$ components only appear in terms of order ε^1 (as damping is assumed to be small), substituting Eqs. (30) into the equation of motion will result in an overall order of accuracy of ε^1.

Next, we substitute Eqs. (30) into the resonant equation of motion for the the first mode, Eq. (11), which may be written

$$\ddot{u}_1 + \omega_{n1}^2 u_1 + N_{u,1} = 0\,, \tag{31}$$

where $N_{u,1}$ is the first element of $\mathbf{N}_u$. Since we are interested in the onset of instability of the zero-amplitude solution we can consider u_1 to be small. Hence we may eliminate terms that are composed of the product of more than one component of u_{1p} and u_{1m}. From this, and using Eq. (17), we may write Eq. (31) as

$$\ddot{u}_1 + \omega_{n1}^2 u_1 + 2\zeta\omega_{n1}\dot{u}_1 + \frac{3\alpha}{m}\left(2u_{2p}u_{2m}u_1 + u_{1p}u_{2m}^2 + u_{1m}u_{2p}^2\right) = 0\,, \tag{32}$$

which, using Eqs. (28) and (30), may be written

$$\begin{aligned}&\left[\mathrm{j}2\Omega\left(U'_{1p} + \zeta\omega_{n1}U_{1p}\right) + \left(\omega_{n1}^2 - \Omega^2\right)U_{1p} + \frac{3\alpha}{m}\left(2U_{2p}U_{2m}U_{1p} + U_{2p}^2U_{1m}\right)\right]\mathrm{e}^{+\mathrm{j}\Omega t}\\ &\quad - \left[\mathrm{j}2\Omega\left(U'_{1m} + \zeta\omega_{n1}U_{1m}\right) - \left(\omega_{n1}^2 - \Omega^2\right)U_{1m} - \frac{3\alpha}{m}\left(2U_{2p}U_{2m}U_{1m} + U_{2m}^2U_{1p}\right)\right]\mathrm{e}^{-\mathrm{j}\Omega t} = 0\,.\end{aligned} \tag{33}$$

It can be seen that Eq. (33) may be written in the form of Eq. (19). Therefore, the contents for the square brackets in Eq. (33) may each be equated to zero, and written as

$$U'_{1p} = \frac{\mathrm{j}}{2\Omega}\left[\left(\omega_{n1}^2 - \Omega^2\right)U_{1p} + \frac{3\alpha}{m}\left(2U_{2p}U_{2m}U_{1p} + U_{2p}^2U_{1m}\right)\right] - \zeta\omega_{n1}U_{1p}\,, \tag{34a}$$

$$U'_{1m} = \frac{-\mathrm{j}}{2\Omega}\left[\left(\omega_{n1}^2 - \Omega^2\right)U_{1m} + \frac{3\alpha}{m}\left(2U_{2p}U_{2m}U_{1m} + U_{2m}^2U_{1p}\right)\right] - \zeta\omega_{n1}U_{1m}\,. \tag{34b}$$

We now let $\mathbf{U}'_1 = \mathbf{f}\left(\mathbf{U}_1\right)$, where $\mathbf{U}_1 = [U_{1p}\,,\, U_{1m}]^T$ such that

$$\mathbf{f}\left(\mathbf{U}_1\right) = \frac{\mathrm{j}}{2\Omega}\begin{pmatrix}\mathrm{j}2\Omega\zeta\omega_{n1}U_{1p} + \left(\omega_{n1}^2 - \Omega^2\right)U_{1p} + \dfrac{3\alpha}{m}\left(2U_{2p}U_{2m}U_{1p} + U_{2p}^2U_{1m}\right)\\ \mathrm{j}2\Omega\zeta\omega_{n1}U_{1m} - \left(\omega_{n1}^2 - \Omega^2\right)U_{1m} - \dfrac{3\alpha}{m}\left(2U_{2p}U_{2m}U_{1m} + U_{2m}^2U_{1p}\right)\end{pmatrix}. \tag{35}$$

We then use $\bar{\mathbf{U}}_1$ to denote $\mathbf{U}_1$ at equilibrium, and $\varepsilon\hat{\mathbf{U}}_1$ to denote a small perturbation. Hence, applying a small perturbation from the equilibrium to $\mathbf{U}_1$, we may write

$$\mathbf{U}_1' = \bar{\mathbf{U}}_1' + \varepsilon\hat{\mathbf{U}}_1' = \mathbf{f}\left(\bar{\mathbf{U}}_1 + \varepsilon\hat{\mathbf{U}}_1\right) = \mathbf{f}\left(\bar{\mathbf{U}}_1\right) + \varepsilon\mathbf{f}_{\mathbf{U}_1}\left(\bar{\mathbf{U}}_1\right)\hat{\mathbf{U}}_1 + \mathcal{O}\left\{\varepsilon^2\right\}, \tag{36}$$

where we have used a Taylor expansion and $\mathbf{f}_{\mathbf{U}_1}$ is the derivative of $\mathbf{f}$ with respect to $\mathbf{U}_1$. Using $\bar{\mathbf{U}}_1' = \mathbf{f}\left(\bar{\mathbf{U}}_1\right)$, we may use Eq. (36) to make the order ε^1 approximation

$$\hat{\mathbf{U}}_1' \approx \mathbf{f}_{\mathbf{U}_1}\left(\bar{\mathbf{U}}_1\right)\hat{\mathbf{U}}_1\,. \tag{37}$$

From Eq. (37) it can be seen that if the real parts of the eigenvalues of $\mathbf{f}_{\mathbf{U}_1}$ are positive, the solution is unstable. The eigenvalues may be calculated by finding $\mathbf{f}_{\mathbf{U}_1}$ from Eq. (35) as

$$\mathbf{f}_{\mathbf{U}_1} = \frac{\mathrm{j}}{2m\Omega}\begin{bmatrix} \mathrm{j}2m\Omega\zeta\omega_{n1} + \left(\omega_{n1}^2 - \Omega^2\right)m + 6\alpha U_{2p}U_{2m} & 3\alpha U_{2p}^2 \\ -3\alpha U_{2m}^2 & \mathrm{j}2m\Omega\zeta\omega_{n1} - \left(\omega_{n1}^2 - \Omega^2\right)m - 6\alpha U_{2p}U_{2m} \end{bmatrix}. \tag{38}$$

We may now use Eq. (38) to calculate the eigenvalues $\lambda_{1,2}$ as

$$\lambda_{1,2} = -\zeta\omega_{n1} \pm \frac{\sqrt{\left[3\alpha U_2^2\right]^2 - \left[4m\left(\omega_{n1}^2 - \Omega^2\right) + 6\alpha U_2^2\right]^2}}{8m\Omega}\,. \tag{39}$$

As instability, i.e. internal resonance, will occur when $\Re\{\lambda\} > 0$, we are interested in the region defined by

$$\Re\left\{\sqrt{\left[3\alpha U_2^2\right]^2 - \left[4m\left(\omega_{n1}^2 - \Omega^2\right) + 6\alpha U_2^2\right]^2}\right\} > 8m\Omega\zeta\omega_{n1}\,. \tag{40}$$

When $\Omega^2 > \omega_{n1}^2 + \frac{3\alpha}{4m}U_2^2$ then the left-hand-side of Eq. (40) is non-zero and we may write

$$\left(\frac{3\alpha}{4m}U_2^2\right)^2 > \left(2\Omega\zeta\omega_{n1}\right)^2 + \left(\omega_{n1}^2 - \Omega^2 + \frac{6\alpha}{4m}U_2^2\right)^2. \tag{41}$$

This defines the region where a zero-amplitude response in the first mode is unstable. Hence a mixed-mode response, containing both u_1 and u_2 must emerge from the boundary of this region.

Figure 3 shows the internally-resonant regions for the example system. The light-red shaded area represents the internally-resonant region, as predicted using Eq. (41). It can be seen that all second-mode-only forced responses within this region are unstable (represented by a solid-red line) and the points at which these responses intersect the boundary of the region coincide with bifurcations onto mixed-mode responses. This is representative of the triggering of an internally resonant response, i.e. the first mode is an NDE mode exhibiting a response due to internal interactions with the second, directly forced, mode.

Conclusions

In this paper we have shown how the backbone curves of a system can be used to determine whether internal resonance may be observed. We have also introduced a method for finding the regions in which internally resonant behaviour may be triggered. This method is derived using the second-order normal from technique, which may also be used to find the backbone curves of the system. As the internally-resonant regions are calculated independently of forcing, they may be used to understand the mechanisms behind the internal resonance for any forcing conditions (assuming the forcing meets the requirements for internal resonance).

This technique may be used to better understand the internally-resonant behaviour of structures such as cables, beams, plates and shells. As the backbone curves and internally-resonant regions may be described

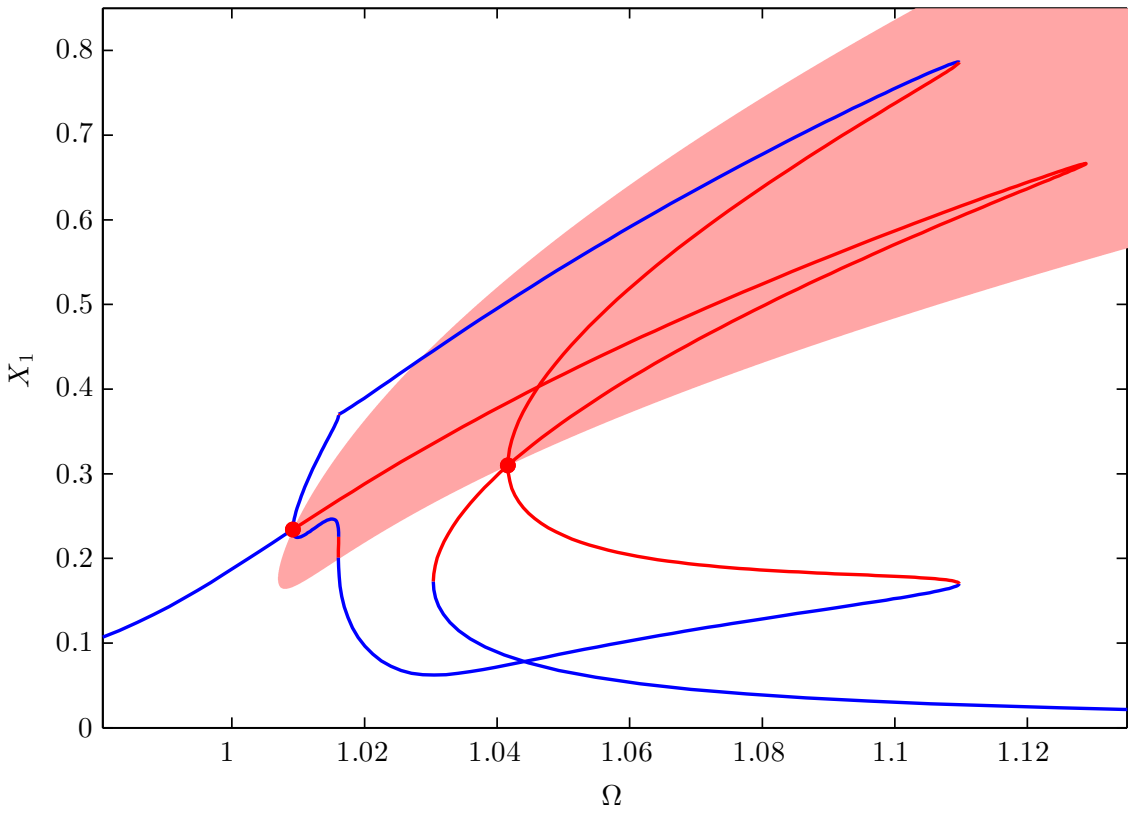

Fig. 3 The forced responses and internally-resonant region for the example system. This is shown in the projection of the forcing frequency, Ω, against the amplitude of displacement of the first mass, X_1. Solid-blue and solid-red lines show stable and unstable forced responses respectively. Large-red dots show the bifurcations from the second-mode-only forced response onto the mixed-mode forced response. The light-red shaded area represents the region in which a second-mode-only response is unstable, and an internal resonance is triggered.

analytically, this approach provides and efficient tool for design and optimisation. The main limitation of the use of the internally-resonant region is that it cannot be used to determine the behaviour of the system in regions where internal resonance has been triggered. For example, a small region at low amplitude may lead to a very large amplitude internally-resonant response. However, the backbone curves may be used to provide some insight into the structure of the internally-resonant response.

References

[1] Hill, T.L., Cammarano, A., Neild, S.A., Wagg, D.J.: (in press) Out-of-unison resonance in weakly-nonlinear coupled oscillators. Proc. R. Soc. A

[2] Cammarano, A., Neild, S.A., Burrow, S.G., Wagg, D.J., Inman, D.J.: Optimum resistive loads for vibration-based electromagnetic energy harvesters with a stiffening nonlinearity. J. Intel. Mat, Syst. Str 25, 1757-1770 (2014)

[3] Lewandowski, R.: On beams membranes and plates vibration backbone curves in cases of internal resonance. Meccanica 31, 323-346 (1996)

[4] Marsico, M.R., Tzanov, V., Wagg, D.J., Neild, S.A., Krauskopf, B.: Bifurcation analysis of a parametrically excited inclined cable close to two-to-one internal resonance. J. Sound Vib. 330, 6023 - 6035 (2011)

[5] Tondl, A, Ruijgrok, T., Verhulst, F., Nabergoj, R.: Autoparametric Resonance in Mechanical Systems. Cambridge University Press, (2000)

[6] Glendinning, P.: Stability, Instability and Chaos: An Introduction to the Theory of Nonlinear Differential Equations. Cambridge University Press, Cambridge Texts in Applied Mathematics (1994)

[7] Kerschen, G., Peeters, M., Golinval, J.C., Vakakis, A.F.: Nonlinear normal modes, Part I: A useful framework for the structural dynamicist. Mech. Syst. Signal Pr. 23, 170 - 194 (2009)

[8] Peeters, M., Viguié, R., Sérandour, G., Kerschen, G., Golinval, J.C.: Nonlinear normal modes, Part II: Toward a practical computation using numerical continuation techniques. Mech. Syst. Signal Pr. 23, 195 - 216 (2009)

[9] Murdock, J.: Normal Forms and Unfoldings for Local Dynamical Systems. Springer, (2002)

[10] Neild, S.A. 2012 Approximate methods for analysing nonlinear structures. In *Exploiting nonlinear behavior in structural dynamics* (ed. D.J. Wagg & L. Virgin), CISM Courses and Lectures 536 pp. 53-109 Vienna: Springer

[11] Cammarano, A., Hill, T.L., Neild, S.A., Wagg, D.J.: Bifurcations of backbone curves for systems of coupled nonlinear two mass oscillator. Nonlinear Dynam. 77, 311–320 (2014)

[12] Neild, S.A., Wagg, D.J.: Applying the method of normal forms to second-order nonlinear vibration problems. Proc. R. Soc. A 467, 1141-1163 (2011)

[13] Xin, Z.F., Neild, S.A., Wagg, D.J., Zuo, Z.X.: Resonant response functions for nonlinear oscillators with polynomial type nonlinearities. J. Sound Vib. 332, 1777 - 1788 (2013)

[14] Doedel, E.J., with major contributions from Champneys, A.R., Fairgrieve, T.F., Kuznetsov, Yu.A., Dercole, F., Oldeman, B.E., Paffenroth, R.C., Sandstede, B., Wang, X.J., Zhang, C.: AUTO-07P: Continuation and Bifurcation Software for Ordinary Differential Equations. Concordia University, Montreal, Canada. http://cmvl.cs.concordia.ca (2008).